

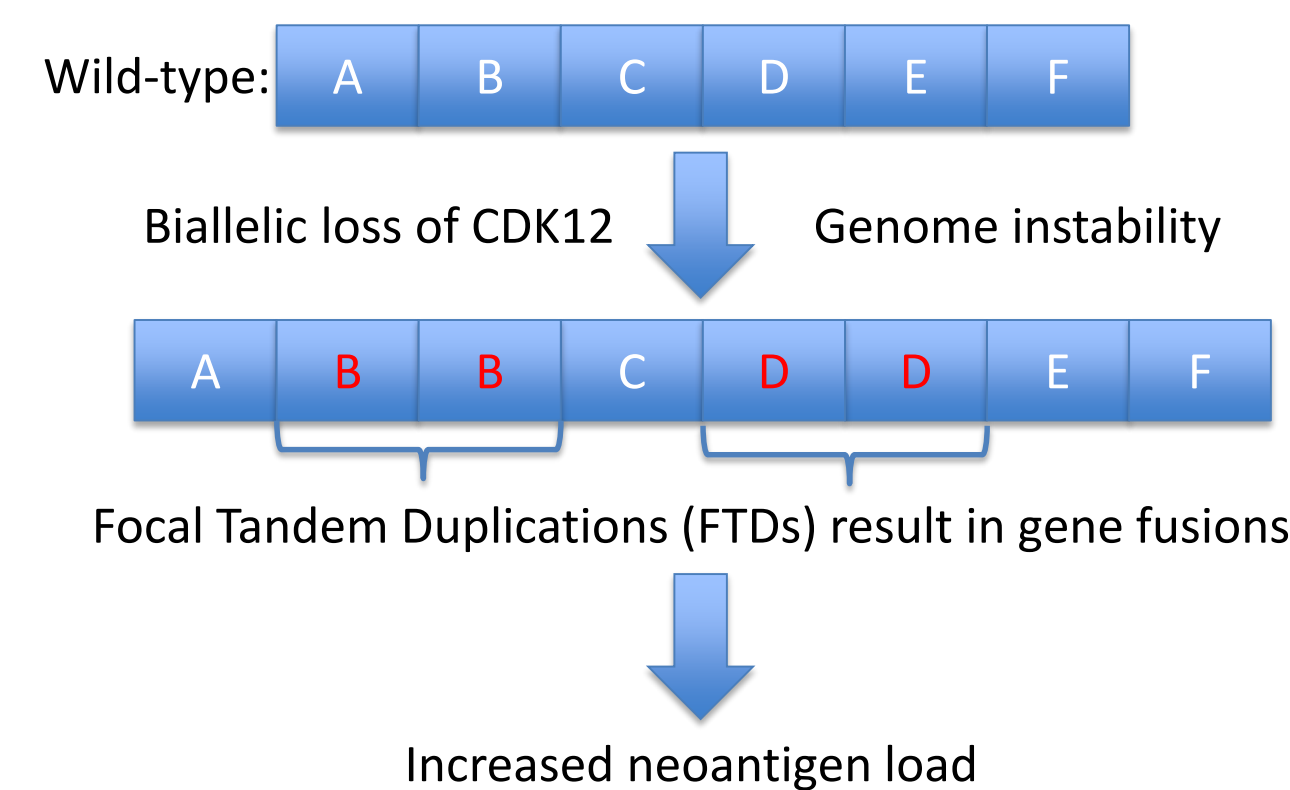
# Fusion-associated neoantigen burden and predicted immunogenicity of CDK12 biallelic loss-of-function tumors vary substantially across cancer types

Andrew Elliott<sup>1</sup>, Phillip Stafford<sup>1</sup>, Jian Zhang<sup>1</sup>, Qing Zhang<sup>1</sup>, Jeff Swensen<sup>1</sup>, Daniel Martin<sup>1</sup>, Joanne Xiu<sup>1</sup>, Zoran Gatalica<sup>1</sup>, Daniel Vaena<sup>2</sup>, Elisabeth Heath<sup>3</sup>, W. Michael Korn<sup>1</sup>  
<sup>1</sup>Caris Life Sciences, Phoenix, AZ; <sup>2</sup>West Cancer Center, Germantown, TN; <sup>3</sup>Wayne State University/Karmanos Cancer Institute, Detroit, MI

Abstract #:3639

## Background

- Biallelic inactivation of CDK12 is associated with a distinct genomic signature of focal tandem duplications (FTDs).<sup>1</sup>
- Gene fusions resulting from CDK12-associated FTDs increase neoantigen load, raising interest in CDK12 as a biomarker of response to immune checkpoint inhibitors (ICIs).



- New treatments are needed for CDK12-altered tumors, which show poor response to PARP inhibition compared to DNA damage response pathway genes.<sup>2</sup>
- Although FTDs have been detected at higher rates in CDK12-altered tumors compared to CDK12 WT tumors for multiple cancer types, fusion-associated neoantigen burden has not been evaluated beyond metastatic castration-resistant prostate cancer.

## Methods

- Retrospective review of a primary cohort of 9024 patients, representing 39 cancer types, whose tumors were profiled with Caris Life Sciences.
- Next-generation sequencing was performed on genomic DNA isolated from formalin-fixed paraffin-embedded tumor samples using the NextSeq platform (Illumina, Inc., San Diego, CA)
- Whole Transcriptome Sequencing was performed on mRNA isolated from a formalin-fixed paraffin-embedded tumor sample using the Illumina NovaSeq platform (Illumina, Inc., San Diego, CA) and Agilent SureSelect Human All Exon V7 bait panel (Agilent Technologies, Santa Clara, CA).
- Fusion topologies were assessed by mapping gene fusion sequences to the reference genome GRCh37/hg19 to identify chromosome number, sense/antisense strand, and genomic breakpoint coordinates for gene-pairs of each fusion event.
- For immune epitope prediction, peptide sequences were translated from fusion transcripts beginning 30 nucleotides (10 amino acids) upstream from the fusion breakpoint; MHC-I binding prediction was performed for all HLA allele/peptide combinations for each tumor using the NetMHCpan v4.0 method in the Immune Epitope Database (IEDB) online resource (<http://tools.iedb.org/mhci/>).
- Pathogenic/likely pathogenic (P/LP) CDK12 alterations included all truncating mutations, fusions, and copy number losses, as well as mutations in the kinase domain. CDK12 biallelic LOF cohort included: 1) tumors with ≥ 2 P/LP CDK12 alterations, or 2) tumors with 1 CDK12 P/LP alteration and ≥ 70% alteration frequency of sequencing reads, which served as a proxy for loss-of-heterozygosity. CDK12 monoallelic LOF cohort included tumors with 1 CDK12 P/LP alteration and < 70% alteration frequency. CDK12 WT cohorts included tumors with no P/LP CDK12 alterations.
- Biomarker and fusion results for a second cohort of 13,416 patient tumors were reviewed for validation of the initial findings.
- Statistical analysis was performed using the Mann-Whitney U test. (\*p<0.05, \*\*p<0.01, \*\*\*p<0.001, \*\*\*\*p<0.0001)

## Results

**Figure 1** – Prevalence of presumed CDK12 biallelic and monoallelic loss-of-function (LOF) across cancer types. Total number of CDK12 biallelic LOF cases noted in parentheses.

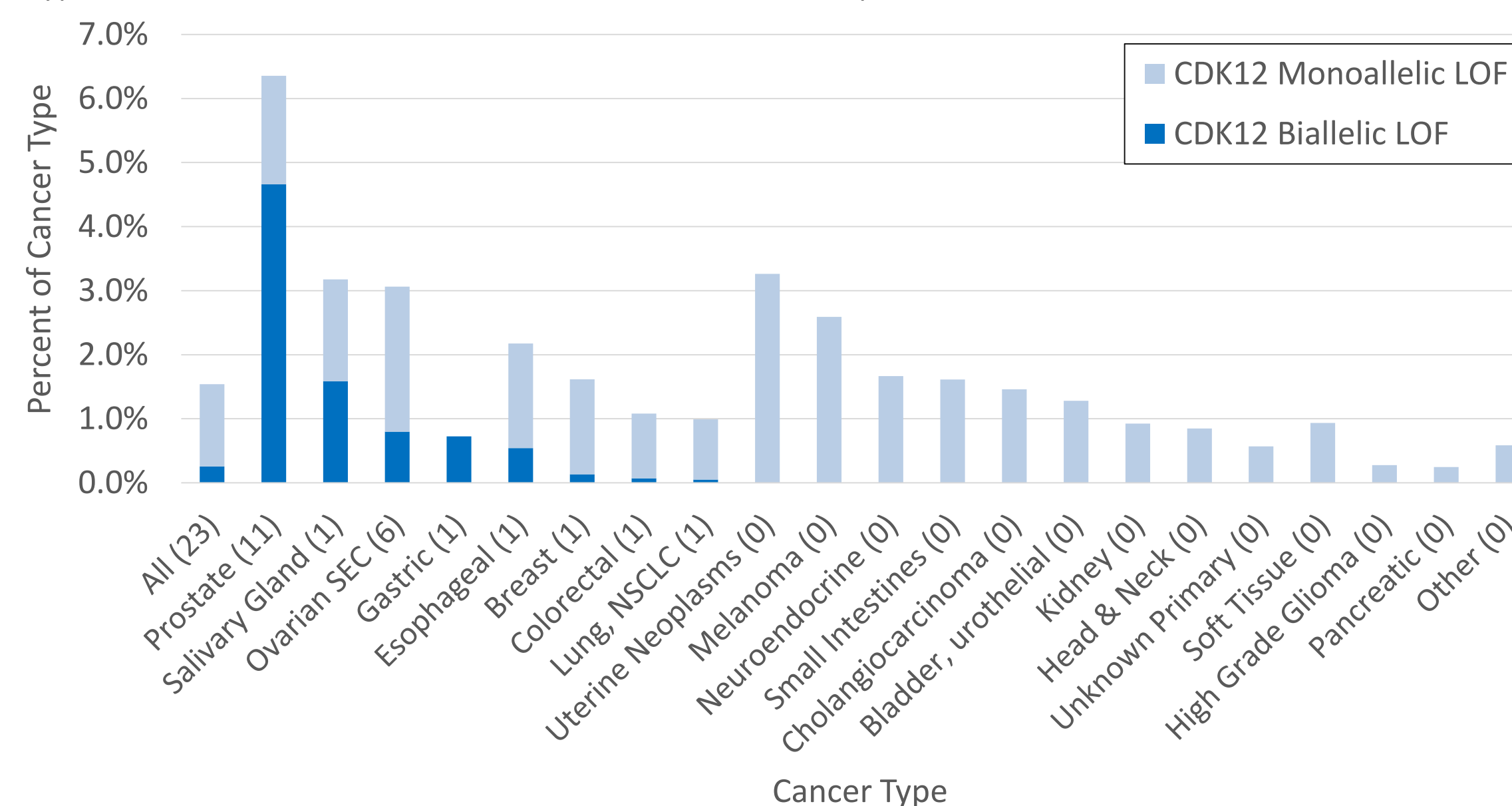


**Table 1** - Clinical characteristics of patients cohorts based on CDK12 allele functional status.

Characteristic	CDK12-MT Biallelic LOF*	CDK12-MT Monoallelic LOF	CDK12-WT
Total, n (%)	29 (0.3%)	116 (1.3%)	8879 (98.4%)
Median age (range)	64 (28-90+) <sup>NS</sup>	65 (34-87)	65 (0-90+)
Sex, n (%)			
Female	11 (37.9%) <sup>NS</sup>	73 (62.9%)	5065 (57.0%)
Male	18 (62.1%)	43 (37.1%)	3814 (43.0%)
Specimen site, n (%)			
Metastatic	12 (41.4%) <sup>NS</sup>	57 (49.1%)	4111 (46.3%)
Primary	17 (58.6%)	59 (50.9%)	4763 (53.6%)
Unclear	0 (0.0%)	0 (0.0%)	5 (0.1%)

\*Includes 6 additional colorectal cases that were tested by WTS for inclusion in the study

**Figure 2** – CDK12 biallelic LOF has a tendency of mutual exclusivity with other genetic driver alterations. (A) Frequency of key genetic driver alteration and Oncoprint. (B) Alterations detected in CDK12 biallelic LOF tumors with tumor type indicated. For tumors with deficient mismatch repair protein expression/microsatellite instability-high (dMMR/MSI-H), recurrent CDK12 frameshift mutations (G1461fs, T1463fs, and Q1291fs) coincide with poly-nucleotide tracts. (Modified graphic generated using OncoPrinter, <https://www.cbioportal.org/oncoprinter>)

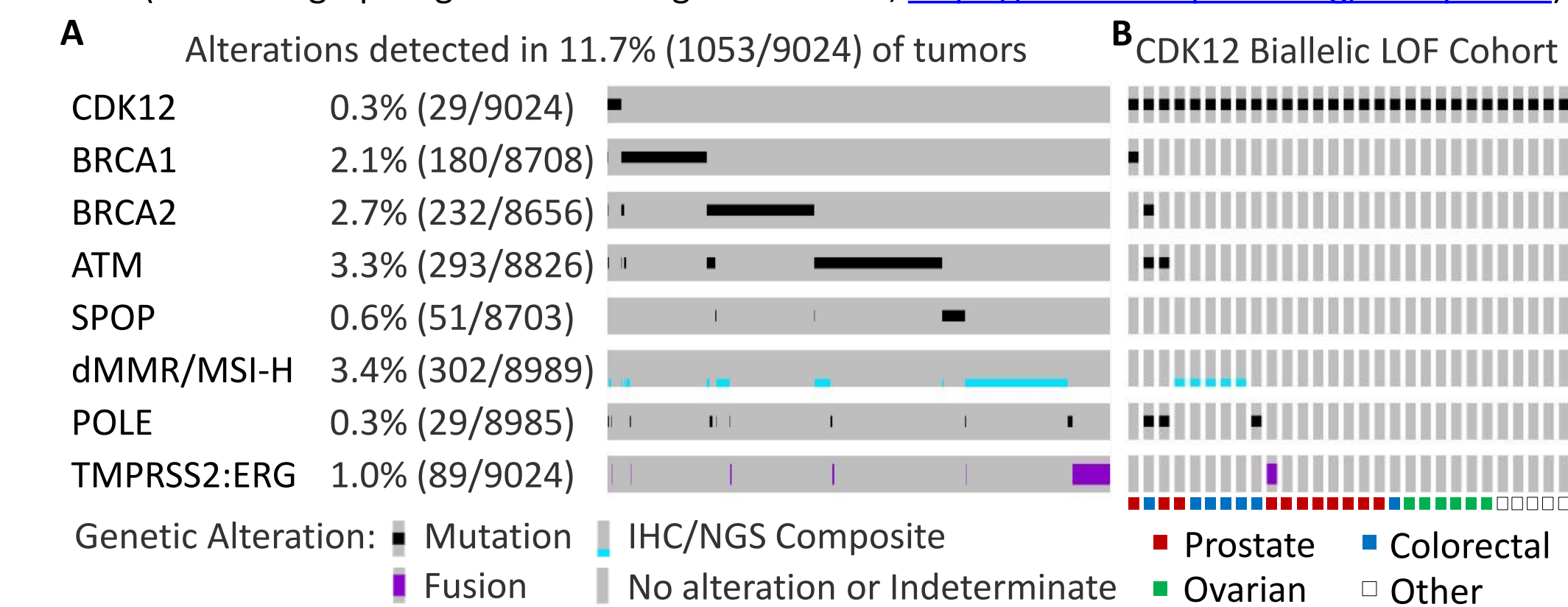


**Figure 3** – Increased gene fusion rate is associated with CDK12 biallelic LOF. (A) Total number of fusion isoforms detected per tumor by CDK12 functional status. (B) For CDK12 biallelic LOF tumors, total number of fusion isoforms detected per tumor by cancer type. Green line indicates cohort mean.

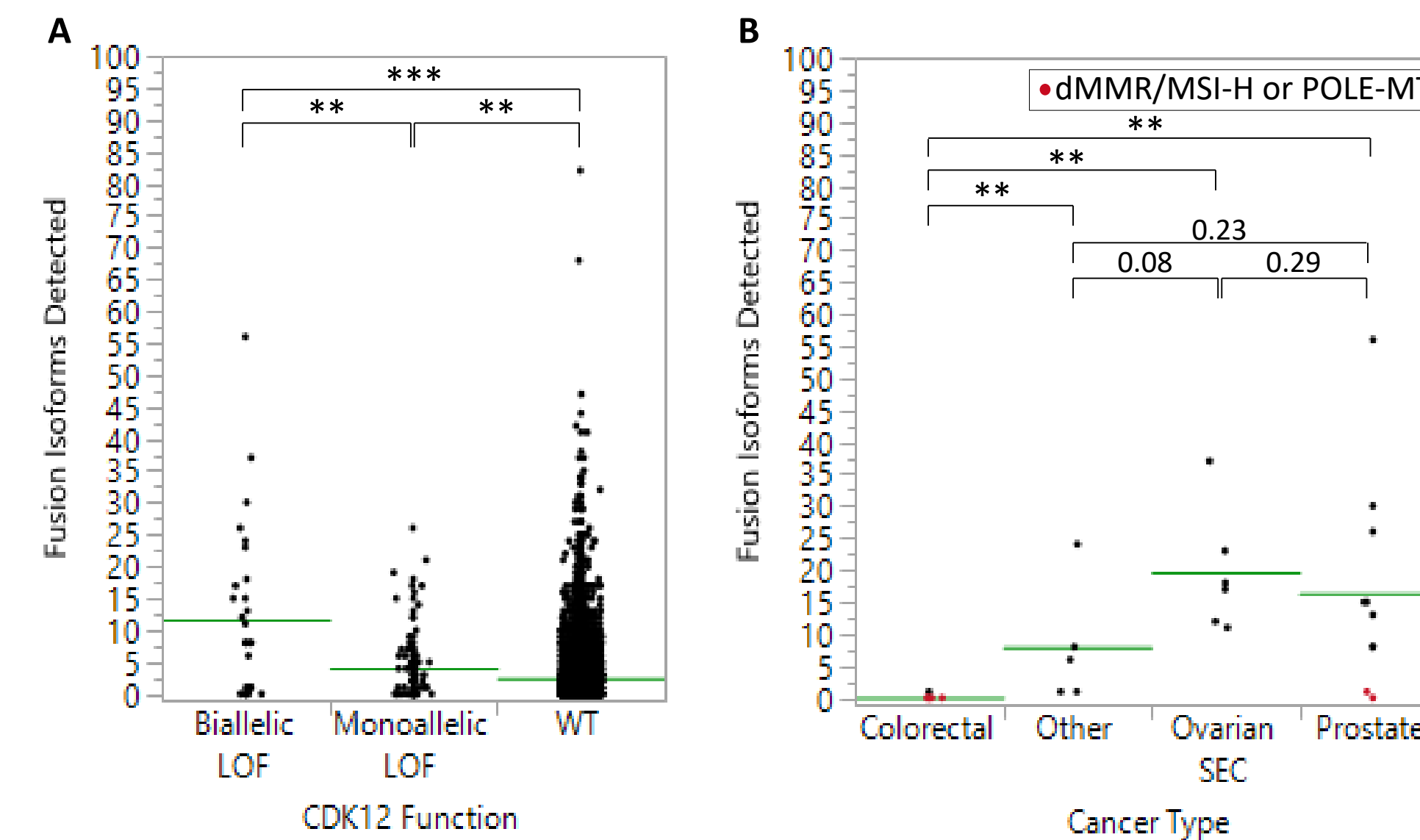


**Figure 4a** – Distribution of fusion topologies based on genomic coordinates of fusion breakpoints. Fusions in CDK12 biallelic LOF tumors are largely derived from duplication events.

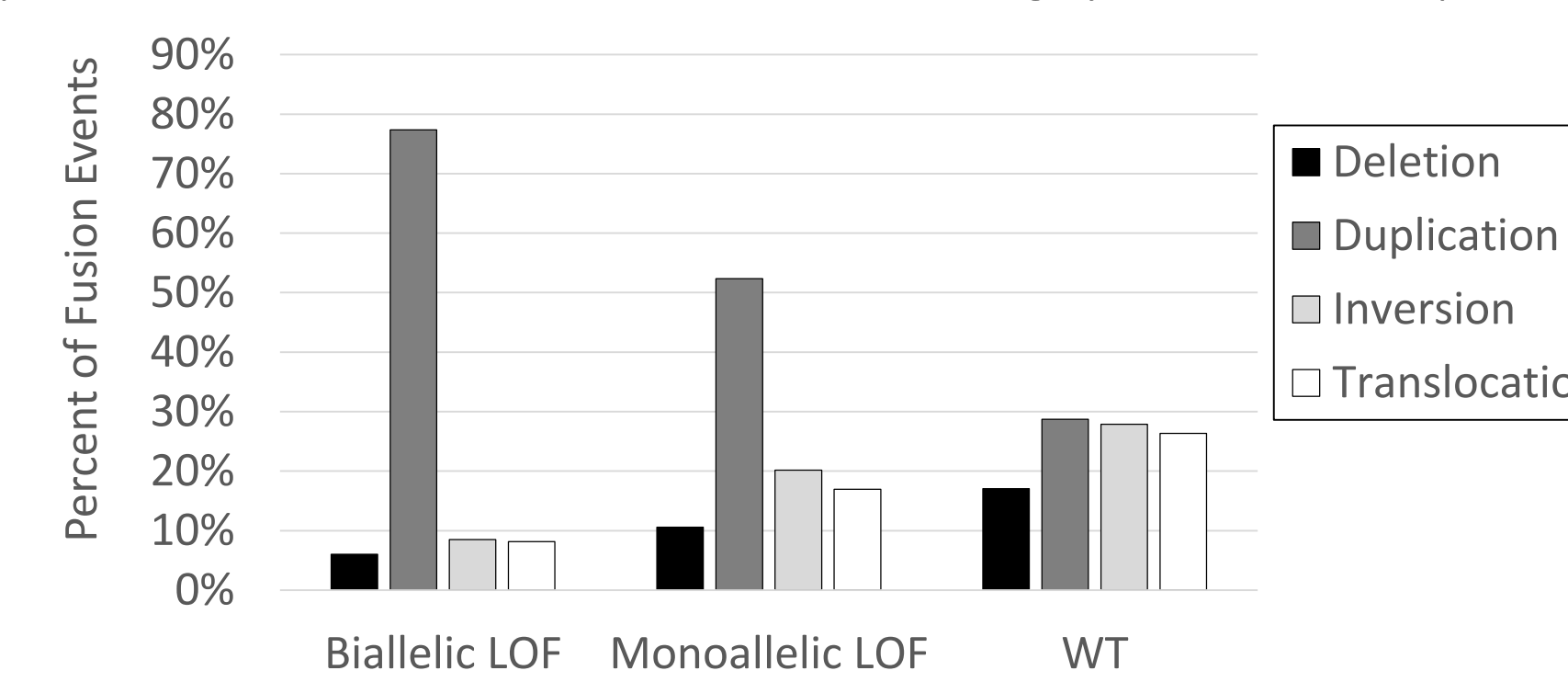


**Figure 4b** – Distribution of breakpoint distances between gene-pairs of fusions with a duplication topology. CDK12 biallelic LOF tumors exhibit a bimodal distribution of breakpoint distances (modes at ~250-500 kb and ~1.0-2.5 Mb), with sizes comparable to that of replication domains. Fusion events detected by WTS in tumors with CDK12 biallelic LOF are representative of the previously reported FTD phenotype.<sup>1</sup>

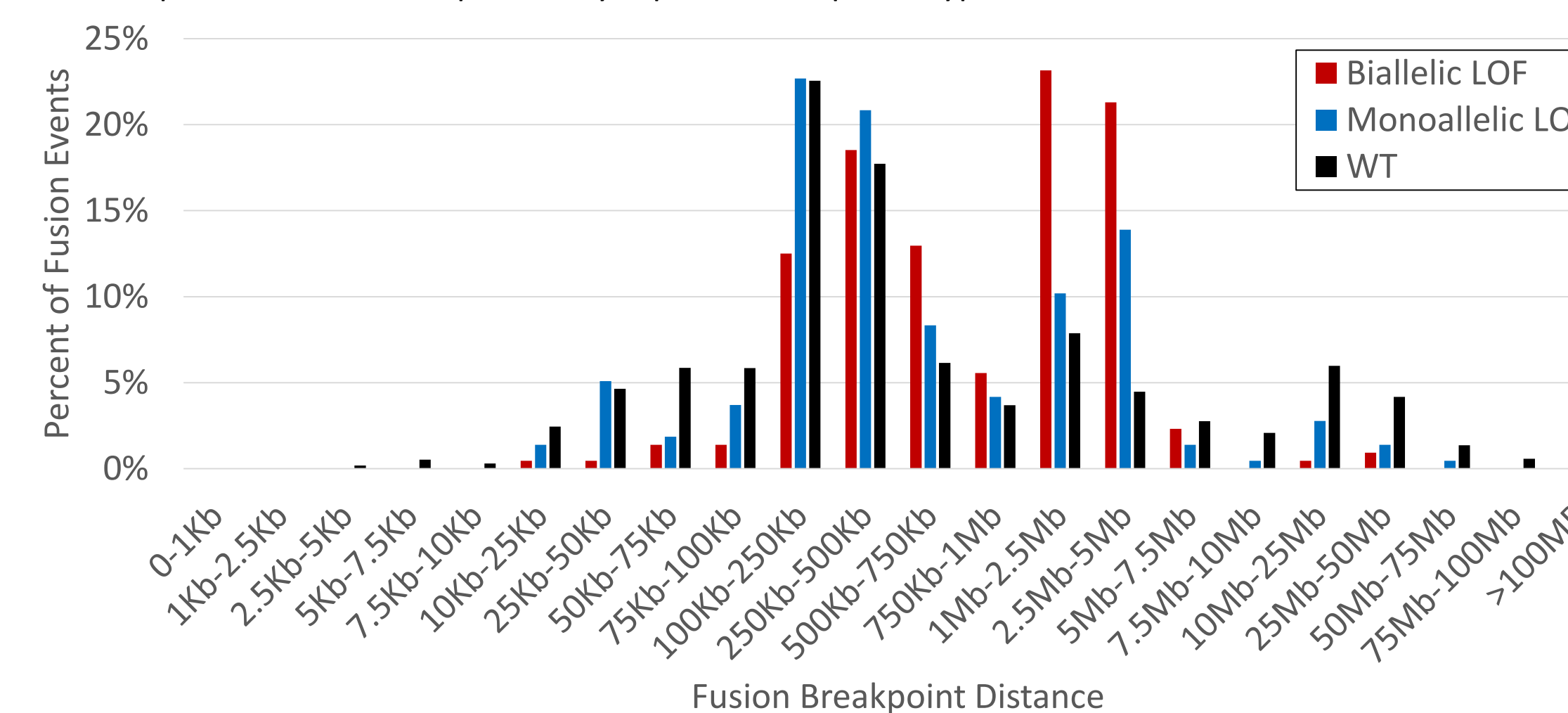


**Figure 5** – Increased fusion-induced neoantigen load is associated with CDK12 biallelic LOF. (A) Total number of fusion-derived peptides with high affinity (IC50 < 50 nm) for MHC-I per tumor. (B) For CDK12 biallelic LOF tumors, total number of fusion-derived high affinity peptides per tumor by cancer type. Green line indicates cohort mean.

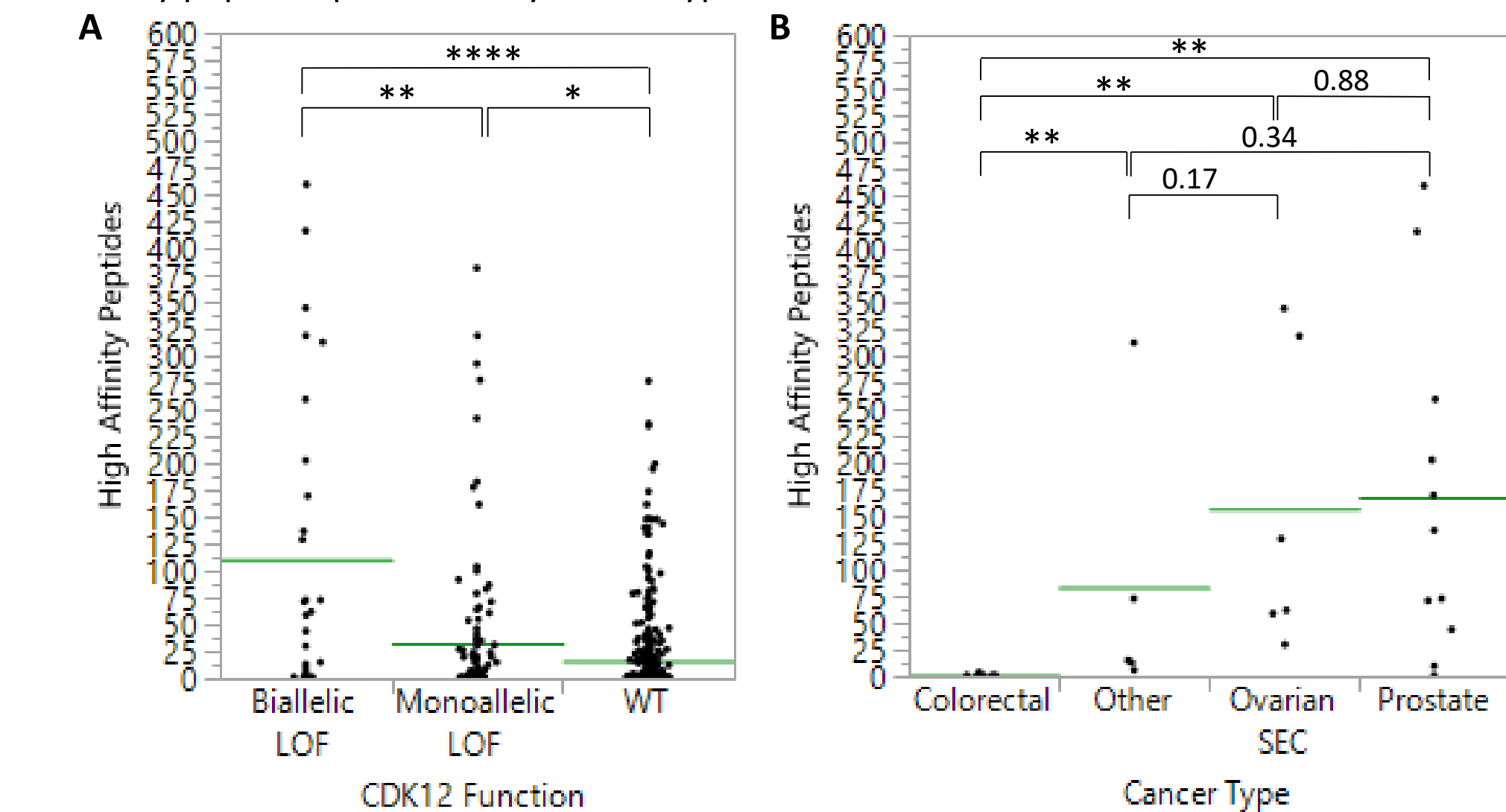
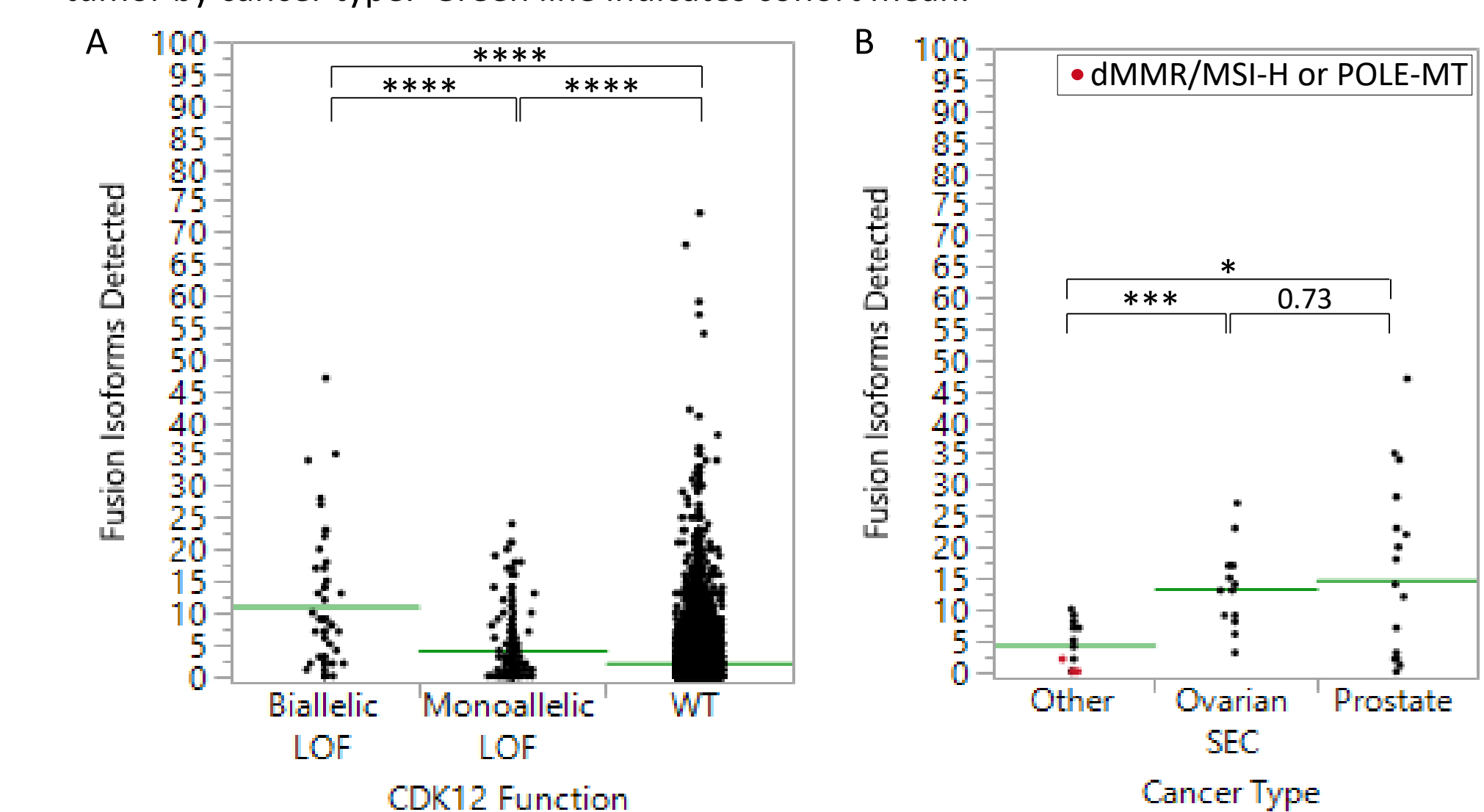


**Figure 6** – Fusion results validated in a separate cohort. (A) From a cohort of over 13,000 patient tumors, total number of fusion isoforms detected per tumor by CDK12 functional status. (B) For CDK12 biallelic LOF tumors, total number of fusion isoforms detected per tumor by cancer type. Green line indicates cohort mean.



## Conclusions

- Fusion rates and predicted neoantigen load varied significantly between CDK12 biallelic LOF tumors across cancer types, highlighting the value of biomarkers with a quantitative, phenotypic and/or immunogenic readout.
- Co-occurrence of dMMR/MSI-High with CDK12 biallelic LOF correlated with a lower fusion rate and recurrent CDK12 frameshift mutations at poly-nucleotide tracts, suggesting CDK12 mutations are a secondary effect in these tumors.
- We propose that fusion rates are linked to CDK12 alterations and may serve as useful biomarker to enhance our ability to identify responders of ICI therapy.

## References

- Wu YM, Ciešlik M, Lonigro RJ, et al. Inactivation of CDK12 Delineates a Distinct Immunogenic Class of Advanced Prostate Cancer. *Cell*. 2018;173(7):1770-1782.e14. doi:10.1016/j.cell.2018.04.034
- Abida W, Campbell D, Patnaik A, et al. Non-BRCA DNA Damage Repair Gene Alterations and Response to the PARP Inhibitor Rucaparib in Metastatic Castration-Resistant Prostate Cancer: Analysis From the Phase II TRITON2 Study. *Clin Cancer Res*. 2020;10.1158/1078-0432.CCR-20-0394. doi:10.1158/1078-0432.CCR-20-0394